An Efficient Algorithm for Analyzing Large-Scale Microstrip Structures Using Adaptive Integral Method Combined with Discrete Complex-Image Method

Feng Ling, *Student Member, IEEE*, Chao-Fu Wang, *Member, IEEE*, and Jian-Ming Jin, *Senior Member, IEEE*

***Abstract*—An efficient algorithm combining the adaptive integral method and the discrete complex-image method (DCIM) is presented in this paper for analyzing large-scale microstrip structures. The arbitrarily shaped microstrips are discretized using triangular elements with Rao–Wilton–Glisson basis functions. These basis functions are then projected onto a rectangular grid, which enables the calculation of the resultant matrix–vector product using the fast Fourier transform. The method retains the advantages of the well-known conjugate-gradient fast-Fourier-transform method, as well as the excellent modeling capability offered by triangular elements. The resulting algorithm has the memory requirement proportional to $O(N)$ and the operation count for the matrix–vector multiplication proportional to $O(N \log N)$, where N denotes the number of unknowns. The required spatial Green's functions are computed efficiently using the DCIM, which further speeds up the algorithm. Numerical results for some microstrip circuits and a microstrip antenna array are presented to demonstrate the efficiency and accuracy of this method.**

***Index Terms*—Adaptive integral method, fast Fourier transform, Green's function, microstrip, method of moments.**

I. Introduction

ACCURATE and efficient electromagnetic simulations are essential for the design of microstrip structures, such as microwave integrated circuits, microstrip antennas, and microstrip reflectarrays. A variety of numerical methods have been developed in the past for this purpose. Among all these methods, the method of moments (MoM) is a popular choice because it discretizes only the microstrips, thus leading to a minimum number of unknowns. The MoM analysis can be carried out either in the spectral domain [1], [2] or spatial domain [3]–[6]. The spectral-domain MoM has an advantage in that the spectral Green's functions can be obtained and calculated easily. However, the basis and testing functions are restricted to those that have analytical Fourier transforms, such as the rooftop and piecewise sinusoidal basis functions. Furthermore, the evaluation of the doubly infinite integrals in the matrix elements is cumbersome and time consuming. The spatial-domain MoM has no restriction on the basis and testing functions. However, it requires the evaluation of the Sommerfeld integral associated with the spatial Green's functions. Several different techniques have been developed for this evaluation. One such technique is called the discrete complex-image method (DCIM). This method circumvents the numerical evaluation of the Sommerfeld integral and yields the closed-form solution [7], [8], which has been employed to analyze microstrip structures [3], [4]. The preferred choice of basis functions for the spatial-domain MoM is the one developed by Rao *et al.* [9], which is now commonly known as the Rao–Wilton–Glisson (RWG) basis function, because it provides a great capability to model arbitrarily shaped microstrip structures.

To simulate a large-scale electromagnetic problem, it is often necessary to employ a large number of unknowns. For the conventional MoM, whether in the spectral or spatial domain, the memory requirement is always proportional to $O(N^2)$, where N denotes the number of unknowns. This requirement can easily become prohibitive even on the most powerful computers. Even if the memory permits, the computing time can become very excessive because direct matrix inversion solvers, such as Gaussian elimination and *LU* decomposition methods, require $O(N^3)$ floating-point operations. When an iterative solver such as the conjugate gradient (CG) method is employed for solving the MoM matrix equation, the operation count is $O(N^2)$ per iteration because of the need to evaluate the matrix–vector product. This operation count is still too high for an efficient simulation.

To make the iterative method more efficient, it is necessary to speed up the matrix–vector multiplication. By exploiting the translational invariance of the Green's function, the matrix–vector product can be computed using the fast Fourier transform (FFT). When this is combined with the CG method, the resulting algorithm is called the conjugate-gradient fast-Fourier-transform (CGFFT) method [10]–[13]. The use of the FFT reduces the operation count to $O(N \log N)$ per iteration. However, the method works only when the structure is modeled with uniform rectangular grids, which necessitates a staircase approximation in the modeling of an arbitrary geometry. This is often considered as the most serious drawback of

Manuscript received March 30, 1998. This work was supported by the Air Force Office of Scientific Research under a grant via the Multidisciplinary University Research Initiative Program under Contract F49620-96-1-0025, by the Office of Naval Research under Grant N00014-95-1-0848, and by the National Science Foundation under Grant NSF ECE 94-57 735.

The authors are with the Center for Computational Electromagnetics, Department of Electrical and Computer Engineering, University of Illinois at Urbana-Champaign, Urbana, IL 61801-2991 USA.

Publisher Item Identifier S 0018-9480(00)03751-0.

the CGFFT method. To model an arbitrary geometry accurately, one has to use triangular elements. However, the triangular discretization does not allow the application of the FFT to speed up the matrix–vector multiplication. One approach is to use the fast multipole method (FMM), which was first developed for free-space problems [14] and then extended to microstrip problems [15]–[18]. Another approach is to project triangular elements onto uniform grids using either the sparse-matrix/canonical grid method [19], the precorrected-FFT method [20], or the adaptive integral method (AIM) [21]–[23], which, thus far, has only been applied to the free-space problems.

In this paper, the AIM is extended to the analysis of large-scale microstrip structures. The arbitrarily shaped microstrips are first discretized using triangular elements with the RWG basis functions. The basis functions are then translated onto a rectangular grid. This enables the utilization of the FFT to carry out the matrix–vector multiplication. The method retains the advantages of the traditional CGFFT method, as well as the excellent modeling capability offered by triangular elements. The resulting algorithm has the memory requirement proportional to $O(N)$ and the operation count for the matrix–vector multiplication proportional to $O(N \log N)$. The required spatial-domain Green's functions are computed efficiently using the DCIM, which further speeds up the algorithm. Numerical results for some microstrip circuits and a large microstrip antenna array are presented to demonstrate the efficiency and accuracy of this method.

II. Formulation

In this section, we first discuss the mixed-potential integral-equation (MPIE) formulation combined with the DCIM. We then discuss the details of the AIM for the microstrip problems. Finally, we briefly mention the approach used to calculate radiation patterns and extract S-parameters to be presented in this paper.

A. MPIE Formulation

Consider a general microstrip structure residing on an infinite substrate having relative permittivity ϵ_r and thickness h. The microstrips are in the x–y plane and excited by an applied field $\mathbf{E}^a$. The induced current on the microstrips can be found by solving the following MPIE:

$$j\omega\mu_0\hat{z} \times \left[\mathbf{A}(\mathbf{r}) + \frac{1}{k_0^2}\nabla\Phi(\mathbf{r})\right] = \hat{z} \times \mathbf{E}^a(\mathbf{r}) \tag{1}$$

where the vector and scalar potentials can be expressed as

$$\mathbf{A}(\mathbf{r}) = \iint_S \bar{\mathbf{G}}_A(\mathbf{r},\mathbf{r}') \cdot \mathbf{J}(\mathbf{r}')\, ds' \tag{2}$$

$$\Phi(\mathbf{r}) = \iint_S G_q(\mathbf{r},\mathbf{r}')\nabla' \cdot \mathbf{J}(\mathbf{r}')\, ds' \tag{3}$$

in which $\bar{\mathbf{G}}_A$ and G_q denote the Green's functions for the magnetic vector and electric scalar potentials, respectively. Denote $\mathbf{G}_A^{xx}$, the xx-component of $\bar{\mathbf{G}}_A$, as G_a. The Green's functions G_a and G_q can be expressed as an inverse Hankel transform of their spectral-domain counterparts

$$G_{a,q}(\rho) = \int_{-\infty}^{+\infty} \tilde{G}_{a,q}(k_\rho) H_0^{(2)}(k_\rho\rho) k_\rho\, dk_\rho \tag{4}$$

where the integral is commonly known as the Sommerfeld integral. The analytical solution of (4) is generally not available, and the numerical integration of the Sommerfeld integral is time consuming. This problem can be alleviated using the DCIM [7], [8], which yields closed-form expressions. The DCIM extracts the quasi-dynamic and surface-wave contributions from the spectral-domain Green's function and approximates the remainder as complex images by Prony's method. The spatial-domain Green's function can then be obtained analytically using the Sommerfeld identity.

To solve the integral equation (1), one first divides the microstrips into triangular elements and then expands the current on the microstrips using the RWG basis function $\mathbf{f}_n(\mathbf{r})$ [9]

$$\mathbf{J} = \sum_{n=1}^{N} I_n \mathbf{f}_n(\mathbf{r}) \tag{5}$$

where N is the number of unknowns. Applying Galerkin's method to (1) results in the matrix equation

$$ZI = V \tag{6}$$

in which the impedance matrix Z and vector V have the elements given by

$$Z_{mn} = j\omega\mu_0 \iint_{T_m} \iint_{T_n} \left[\mathbf{f}_m(\mathbf{r}) \cdot \mathbf{f}_n(\mathbf{r}') G_a(\mathbf{r},\mathbf{r}') - \frac{1}{k_0^2}\nabla \cdot \mathbf{f}_m(\mathbf{r})\nabla' \cdot \mathbf{f}_n(\mathbf{r}') G_q(\mathbf{r},\mathbf{r}')\right] d\mathbf{r}'\, d\mathbf{r} \tag{7}$$

and

$$V_m = \iint_{T_m} \mathbf{E}^a(\mathbf{r}) \cdot \mathbf{f}_m(\mathbf{r})\, d\mathbf{r} \tag{8}$$

where T_m and T_n denote the support of $\mathbf{f}_m$ and $\mathbf{f}_n$, respectively.

B. AIM Algorithm

For a large-scale problem, the memory demand for the storage of matrix Z and the computing time to solve (6) can become very excessive when either direct matrix inversion solvers, such as Gaussian elimination and *LU* decomposition methods, or iterative solvers, such as the CG method, are employed directly. For example, an iterative solver requires $O(N^2)$ operations per iteration for the matrix–vector multiplication. To employ AIM to accelerate the matrix–vector multiplication, one first encloses the whole structure in a rectangular region and then recursively subdivides it into small rectangular grids. One then translates the original basis functions on the triangular elements to the rectangular grids. If any one of the Cartesian components of $\mathbf{f}_m(\mathbf{r})$ and $\nabla \cdot \mathbf{f}_m(\mathbf{r})$ is denoted as $\psi_m(\mathbf{r})$, the

impedance matrix element of (7) can be expressed as a linear combination of matrix elements in the form of

$$A_{mn} = \iint_{T_m} \iint_{T_n} \psi_m(\mathbf{r}) g(\mathbf{r}, \mathbf{r}') \psi_n(\mathbf{r}') \, d\mathbf{r}' \, d\mathbf{r} \tag{9}$$

where g can be either G_a or G_q. The $\psi_m(\mathbf{r})$ can be approximated as a combination of the Dirac delta functions on the rectangular grids

$$\psi_m(\mathbf{r}) \simeq \hat{\psi}_m(\mathbf{r}) = \sum_{u=1}^{(M+1)^2} \Lambda_{mu} \delta(\mathbf{r} - \mathbf{r}_{mu}) \tag{10}$$

where Λ_{mu} is the translation coefficient for the basis function $\psi_m(\mathbf{r}), M$ is the order of the translation, and $\mathbf{r}_{mu} = (x_{mu}, y_{mu})$ is the coordinate of the grid. The translation coefficient can be found based on the criterion that the translated basis function produces the same multipole moments as the original basis function

$$\begin{aligned} &\sum_{u=1}^{(M+1)^2} (x_{mu} - x_0)^{q_1} (y_{mu} - y_0)^{q_2} \Lambda_{mu} \\ &\quad = \iint_{T_m} \psi_m(\mathbf{r}) (x - x_0)^{q_1} (y - y_0)^{q_2} \, d\mathbf{r}, \\ &\qquad \text{for } 0 \le q_1, q_2 \le M \end{aligned} \tag{11}$$

where the reference point $\mathbf{r}_0 = (x_0, y_0)$ is chosen as the center of the basis function. The closed-form solution of (11) has been given by Bleszynski *et al.* [22]. Once this translation is found, one can approximate the matrix element of (9) as

$$\hat{A}_{mn} = \sum_{u=1}^{(M+1)^2} \sum_{v=1}^{(M+1)^2} \Lambda_{mu} g(\mathbf{r}_u, \mathbf{r}'_v) \Lambda_{nv}. \tag{12}$$

With the translation formulation given above, one can now rewrite the impedance matrix element with the form of (7) as

$$\begin{aligned} \hat{Z}_{mn} = j\omega\mu_0 \sum_{u=1}^{(M+1)^2} \sum_{v=1}^{(M+1)^2} \Big[&(\Lambda_{x,mu} \Lambda_{x,nv} + \Lambda_{y,mu} \Lambda_{y,nv}) \\ &\cdot G_a(\mathbf{r}_u, \mathbf{r}'_v) \\ &- \frac{1}{k_0^2} \Lambda_{d,mu} \Lambda_{d,nv} \\ &\cdot G_q(\mathbf{r}_u, \mathbf{r}'_v) \Big] \end{aligned} \tag{13}$$

where Λ_x, Λ_y, and Λ_d denote the translation coefficients for the x-component, the y-component, and the divergence of the basis function, respectively. $\hat{Z}_{mn}$ in (13) offers a good accuracy to approximate Z_{mn} in (7) when the basis and testing functions are at a large distance. To utilize (13), the impedance matrix is decomposed into $\hat{Z}$ and a residual matrix R

$$Z = \hat{Z} + R. \tag{14}$$

In matrix form, $\hat{Z}$ can be written as

$$\hat{Z} = j\omega\mu_0 \left[\Lambda_x G_a \Lambda_x^T + \Lambda_y G_a \Lambda_y^T - \frac{1}{k_0^2} \Lambda_d G_q \Lambda_d^T \right] \tag{15}$$

where Λ_x, Λ_y, and Λ_d are sparse matrices with each row containing only $(M+1)^2$ nonzero elements. The translational invariance of G_a and G_q enables the use of the FFT to accelerate the computation of the product of this matrix $\hat{Z}$ with a vector. When the elements with a very small value are neglected, the residual matrix R is very sparse. Only when $\mathbf{f}_m$ and $\mathbf{f}_n$ are very close does R_{mn} has an appreciable value. These features make the algorithm less memory and central processing unit (CPU) time demanding. Employing the CG method as the iterative solver, one can write the matrix–vector multiplication as

$$ZI = \hat{Z}I + RI \tag{16}$$

where $\hat{Z}I$ can be evaluated using the FFT as

$$\begin{aligned} \hat{Z}I = j\omega\mu_0 \Big\{ &\Lambda_x \mathcal{F}^{-1} \Big[\mathcal{F}(G_a) \cdot \mathcal{F}(\Lambda_x^T I) \Big] \\ &+ \Lambda_y \mathcal{F}^{-1} \Big[\mathcal{F}(G_a) \cdot \mathcal{F}(\Lambda_y^T I) \Big] \\ &- \frac{1}{k_0^2} \Lambda_d \mathcal{F}^{-1} \Big[\mathcal{F}(G_q) \cdot \mathcal{F}(\Lambda_d^T I) \Big] \Big\}. \end{aligned} \tag{17}$$

As one can see from the analysis described above, the memory requirement of the AIM is proportional to $O(N)$ due to the sparsity of matrices R and Λ. The CPU time per iteration is dominated by the FFT computation of the matrix–vector product, which is proportional to $O(N \log N)$. In contrast, for the conventional MoM, the CPU time for the matrix fill is of $O(N^2)$ and the CPU time per iteration is also of $O(N^2)$.

C. Excitation and Extraction

The right-hand side of (1) can be different for different problems. For the radiation and circuit problems, one can use a voltage source in the region of the excitation port. As a result, only a few elements of V in (6) are assigned a nonzero value. One can also use a current probe as excitation and, in that case, the applied field $\mathbf{E}^a$ is the field produced by the probe in the absence of the microstrips.

Once the current distribution on the microstrips is obtained, the parameters associated with the current can be extracted. The far-field radiated can be calculated using the standard stationary phase method. A simpler approach is to employ the reciprocity theorem [4]. In this approach, the radiated field in the direction of (θ, ϕ) can be evaluated as

$$E^{\text{rad}}_{\theta,\phi}(\mathbf{r}) = -\frac{j\omega\mu_0 e^{-jk_0 r}}{4\pi r} \iint_S \mathbf{J}(\mathbf{r}') \cdot \mathbf{E}_{\theta,\phi}(\mathbf{r}') \, d\mathbf{r}'. \tag{18}$$

where $\mathbf{E}_{\theta,\phi}(\mathbf{r}')$ are the fields in the presence of the dielectric substrate without the microstrips produced by the θ- and ϕ-polarized electric current elements placed at the observation point in the far zone.

For N-port circuit problems, it is necessary to extract the scattering parameters. In general, N linearly independent excitations are required for the N-port network. The current distribution along the microstrip line associated with the ith port can be expressed as

$$I_i(x) = \frac{1}{\sqrt{Z_{0i}}} \left(a_i e^{-j\beta_i x} - b_i e^{j\beta_i x} \right). \tag{19}$$

Here, port i is assumed to be in the x-direction, and Z_{0i} and β_i are the characteristic impedance and propagation constants of

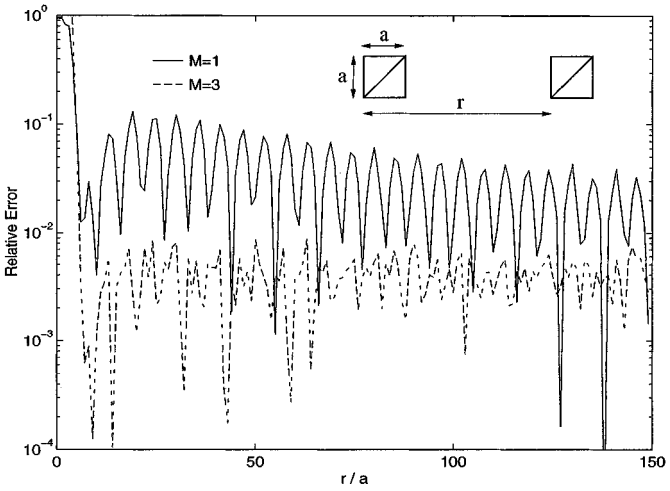

Fig. 1. Relative error in the approximate matrix elements as the function of distance between the basis and testing functions based on the multipole moment approximation. The significant error at small r/a is compensated for by the residual matrix R.

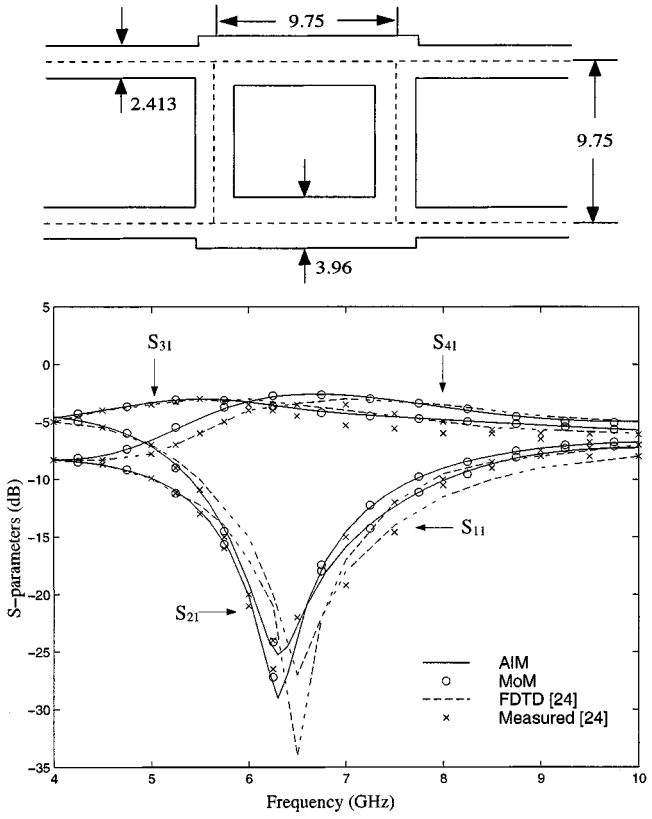

Fig. 2. S-parameters for the branch-line coupler (dimensions in millimeters). $\epsilon_r = 2.2, h = 0.794$ mm.

the microstrip line at port i, respectively, which can be determined in advance. The coefficients a_i and b_i can be extracted by the three-point curve-fitting scheme proposed in [5]. The least-square fit of more current samples can result in a more accurate solution. To obtain correct results, one has to make sure that the sampling points are away from the discontinuity and excitation plane, which also indicates that the microstrip line should be long enough to have the standing-wave pattern. Once

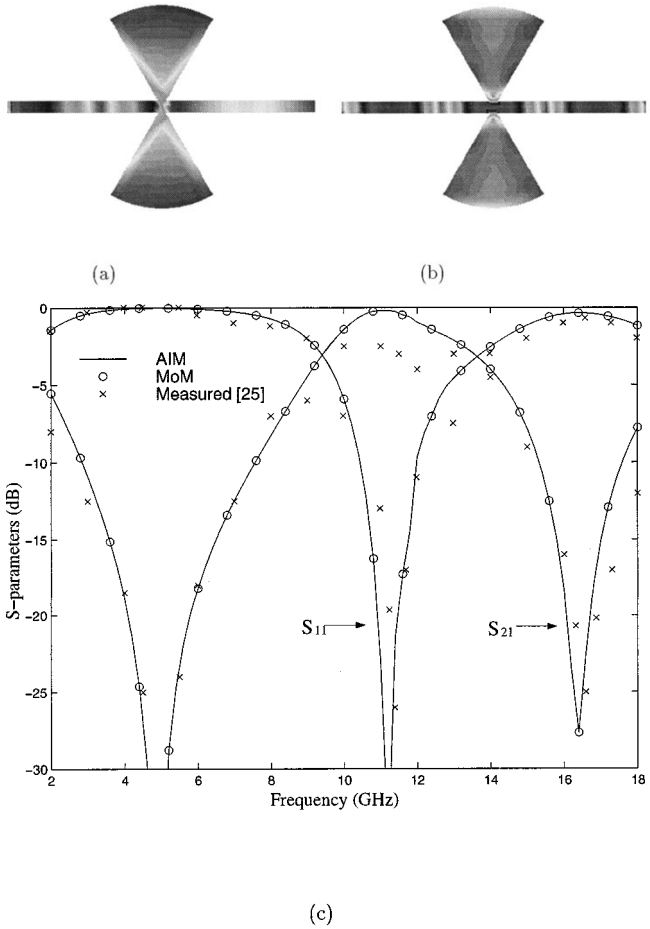

Fig. 3. Current distributions and S-parameters for the radial stub. $\epsilon_r = 10.0, h = 0.635$ mm, width $= 0.6$ mm, radius $= 5.0$ mm, and angle $= 60°$. (a) Current distribution at $f = 8.0$ GHz. (b) Current distribution at $f = 11.0$ GHz. (c) S-parameters.

all a_i's and b_i's are obtained, one can obtain the following equations associated with the S-parameters

$$\sum_{i=1}^{N} a_i S_{ji} = b_j, \qquad j = 1, 2, \cdots, N. \tag{20}$$

Repeat this process N times for N different excitation schemes, one can obtain N^2 equations for all the S-parameters. In some practical cases, the properties of symmetry and reciprocity can be utilized to reduce the number of excitations.

III. Numerical Results

Before we apply the proposed method to realistic problems, the accuracy of this algorithm is examined. As shown in the preceding section, the original impedance matrix element has the form of (7). After the translation based on the multipole moment approximation, the new matrix element with the form of (13) is obtained. To check the accuracy of the translation, we plot the relative error between the matrix elements in (7) and (13) as the function of the distance between the basis and testing functions. The result is given in Fig. 1, where the edge length a is $\lambda/20$ with λ being the wavelength in the medium. The size of the rectangular grid is about $1.2a$. From the figure, one can

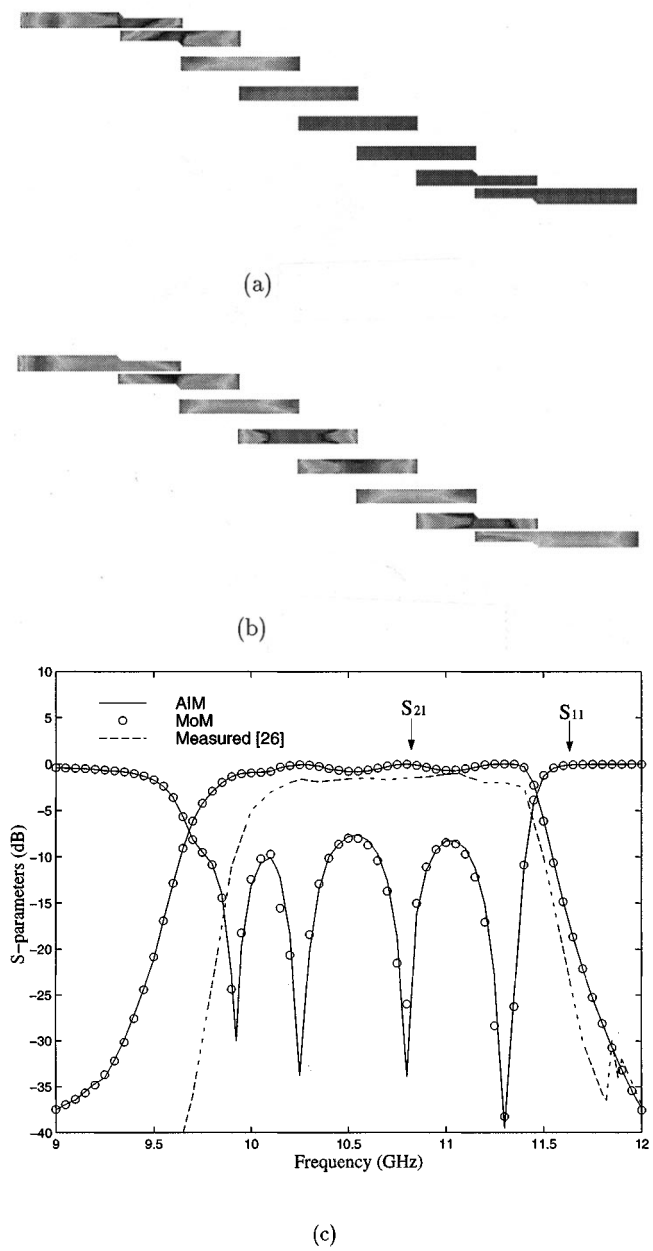

Fig. 4. Current distributions and S-parameters for the parallel-coupled bandpass filter. $\epsilon_r = 10.0, h = 0.635$ mm. (a) Current distribution at $f = 9.0$ GHz. (b) Current distribution at $f = 11.0$ GHz. (c) S-parameters.

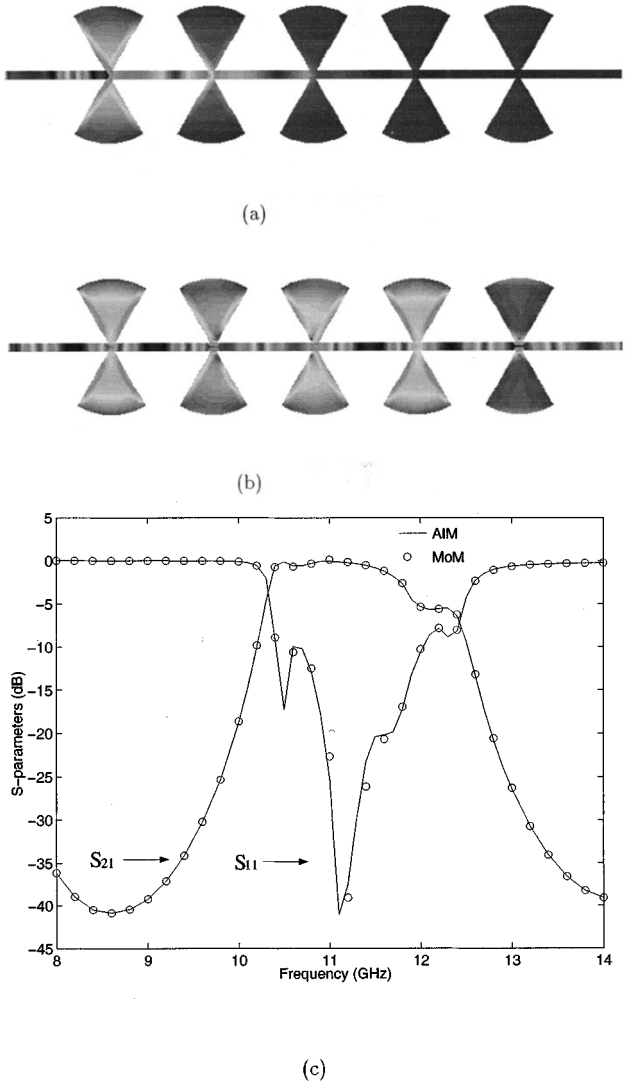

Fig. 5. Current distributions and S-parameters for the cascaded microstrip radial stub. $\epsilon_r = 10.0, h = 0.635$ mm. The spacing between stubs is 7.5 mm. (a) Current distribution at $f = 9.0$ GHz. (b) Current distribution at $f = 11.0$ GHz. (c) S-parameters.

see that the relative error is less than 1% when $M = 3$ and the distance between the basis and testing function is more than five times the grid size. That is the typical situation in the following examples.

We now apply the algorithm to some circuit and antenna problems. The triangular mesh is generated using IDEAS and is then processed for extracting edge information. All the computations are performed on one processor of an SGI Power Challenge (R8000). The iterative solver used is the biconjugate gradient (BCG) method with the diagonal preconditioner. The solution tolerance based on the residual norm is set to 10^{-4}.

We first consider some simple circuits for the verification purpose. The first example is a microstrip branch line coupler, which is a four-port circuit. This structure has been analyzed using the finite-difference time-domain (FDTD) method [24], and it is found difficult for regular FDTD grids to match all of the circuit dimensions exactly. In contrast, all the dimensions in our case are precisely modeled. The numbers of facets and unknowns are 884 and 1206, respectively. The S-parameters obtained are shown in Fig. 2, compared with those calculated by the conventional MoM. Excellent agreement is observed. These results can also be verified by comparison with those of the FDTD method and the measured data in [24]. A slight frequency shift occurs in the FDTD analysis due to its inability to match all the dimensions.

The second example to demonstrate the validity of this method is a microstrip radial stub analyzed in [25]. The substrate has permittivity $\epsilon_r = 10.0$ and thickness $h = 0.635$ mm. To cover the entire frequency band, we consider two different discretizations. The first one is for lower frequencies (below 8 GHz), which involves 364 facets and 457 edges. The microstrip line is truncated at the distance 16.5 mm from the

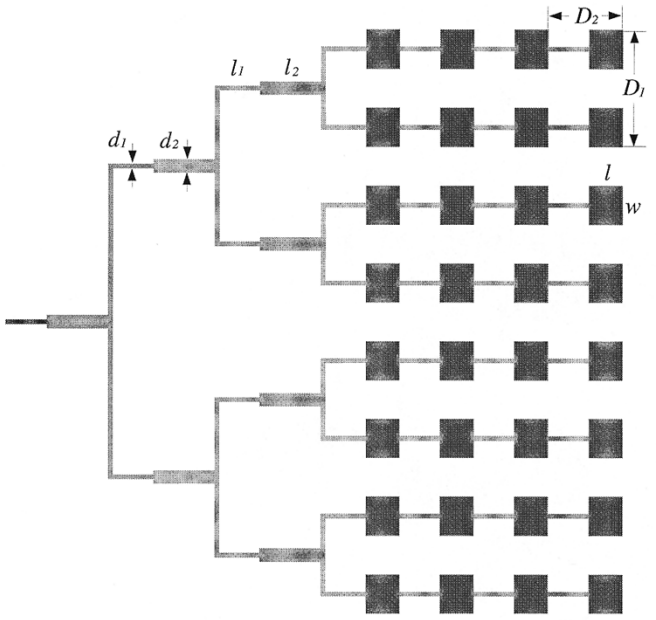

Fig. 6. Current distribution on the microstrip antenna array at the frequency $f = 9.42$ GHz. $\epsilon_r = 2.2, h = 1.59$ mm, $l = 10.08$ mm, $w = 11.79$ mm, $d_1 = 1.3$ mm, $d_2 = 3.93$ mm, $l_1 = 12.32$ mm, $l_2 = 18.48$ mm, $D_1 = 23.58$ mm, $D_2 = 22.40$ mm.

center to make the S-parameter-extraction accurate. The other discretization is for higher frequencies, which involves 862 facets and 1194 edges. To provide physical insight into the performance of the stub, we show the current distribution on the surface at two frequencies: $f = 8.0$ and $f = 11.0$ GHz. The stub is excited at the left-hand-side port, and the other port is left open. We can see that most energy is reflected at $f = 8.0$ GHz, and is transmitted to the other port at $f = 11.0$ GHz. The S-parameters from the proposed method and MoM are given in Fig. 3, which shows a good agreement between two methods. The agreement between our results and the measured data from [25] is also satisfactory.

Next, a parallel-coupled bandpass filter is analyzed. The dimension of the filter is given by [26, Fig. 8.26]. The substrate has permittivity $\epsilon_r = 10.0$ and thickness $h = 0.635$ mm. The numbers of facets and unknowns are 1086 and 1402, respectively. Again, the current distributions are shown at $f = 9.0$ GHz and $f = 11.0$ GHz. The S-parameters of this bandpass filter are shown in Fig. 4. Both MoM and AIM results agree very well. The measured data from [26] are also given in Fig. 4 for comparison. The discrepancy at the low frequency range is believed due to the fabrication error.

The examples above demonstrate the accuracy of this algorithm. Since the structures analyzed are relatively small (the number of unknowns is below 2000), the saving of CPU time is not expected, although the significant memory reduction has been achieved. For large-scale problems, we can predict a substantial reduction of CPU time in both the matrix fill and solve. To illustrate the efficiency of this method, we now consider some large-scale microstrip structures. First, a structure consisting of five radial stubs is analyzed. Each radial stub has the same dimension as in Fig. 3. The spacing between stubs is 7.5 mm. The numbers of facets and unknowns are 3982 and

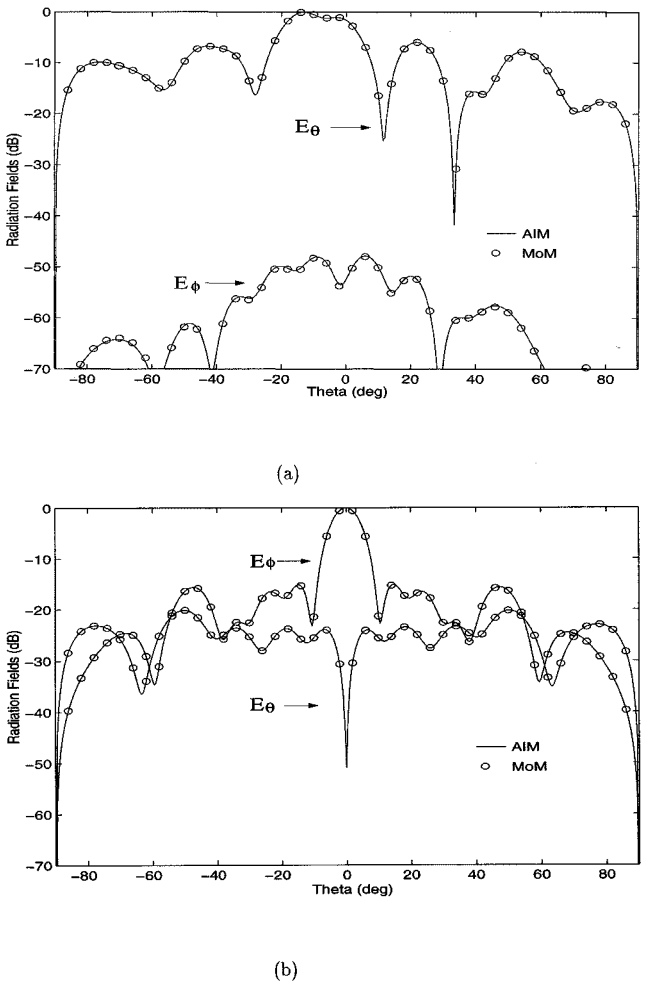

Fig. 7. Radiation patterns of the microstrip antenna array. (a) $\phi = 0°$. (b) $\phi = 90°$.

5580, respectively. The memory requirement is 21 Mbyte and the CPU time per iteration is 1.7 s in the AIM algorithm. In contrast, the conventional MoM requires 250-Mbyte memory and 5.7-s CPU time per iteration. The CPU time for the matrix fill is only 40% of that in the conventional MoM. The S-parameters of this structure are shown in Fig. 5. The current distributions at the two frequencies $f = 9.0$ GHz and $f = 11.0$ GHz are also given in the figure.

Finally, a microstrip antenna array is considered, which involves 6569 facets and 8668 edges. For the conventional MoM, the memory requirement is over 600 Mbyte and the CPU time per iteration is 15.8 s. However, it takes only 22.7 Mbyte and 3.5 sfor the AIM, where the FFT has the dimension of 128 $\times$ 128. The AIM also yields an over 70% reduction in the CPU time for the matrix fill comparing to the conventional MoM. At a frequency of $f = 9.42$ GHz, the current distribution is shown in Fig. 6. The radiation patterns in the two principal planes $\phi = 0°$ and $\phi = 90°$ are given in Fig. 7, which shows excellent agreement between the two solutions.

IV. Conclusion

An efficient algorithm combining the AIM and DCIM is presented for analyzing large-scale microstrip structures.

The MPIE is discretized using the RWG basis functions for expansion and testing. The BCG method is employed to solve the resulting matrix equation. To achieve an efficient solution, we translate the RWG basis functions on a triangular mesh to a rectangular grid. This permits the use of the FFT to carry out the matrix–vector multiplication. The resulting algorithm has the memory requirement proportional to $O(N)$ and the operation count for the matrix–vector multiplication proportional to $O(N \log N)$. The method retains the advantages of the traditional CGFFT method as well as the excellent modeling capability offered by triangular elements. The required spatial Green's functions are computed efficiently using the DCIM, which further speeds up the algorithm. Numerical results for some microstrip circuits and a microstrip antenna array are presented to demonstrate the efficiency and accuracy of this method.

REFERENCES

[1] D. M. Pozar and S. M. Voda, "A rigorous analysis of a microstrip feed patch antenna," *IEEE Trans. Antennas Propagat.*, vol. AP-35, pp. 1343–1350, Dec. 1987.

[2] S. Wu, H. Yang, N. G. Alexopoulous, and I. Wolff, "A rigorous dispersive characterization of microstrip cross and T junctions," *IEEE Trans. Microwave Theory Tech.*, vol. 38, pp. 1837–1844, Dec. 1990.

[3] R. Kipp and C. H. Chan, "Triangular-domain basis functions for full-wave analysis of microstrip discontinuities," *IEEE Trans. Microwave Theory Tech.*, vol. 41, pp. 1187–1194, June 1993.

[4] F. Ling and J. M. Jin, "Scattering and radiation analysis of microstrip antennas using discrete complex image method and reciprocity theorem," *Microwave Opt. Technol. Lett.*, vol. 16, pp. 212–216, Nov. 1997.

[5] D. C. Chang and J. X. Zheng, "Electromagnetic modeling of passive circuit elements in MMIC's," *IEEE Trans. Microwave Theory Tech.*, vol. 40, pp. 1741–1747, Sept. 1992.

[6] K. A. Michalski and C. G. Hsu, "RCS computation of coax-loaded microstrip patch antennas of arbitrary shape," *Electromag.*, vol. 14, pp. 33–62, Jan.–Mar. 1994.

[7] D. G. Fang, J. J. Yang, and G. Y. Delisle, "Discrete image theory for horizontal electric dipole in a multilayer medium," *Proc. Inst. Elect. Eng.*, pt. H, vol. 135, pp. 297–303, Oct. 1988.

[8] Y. L. Chow, J. J. Yang, D. G. Fang, and G. E. Howard, "A closed-form spatial Green's function for the thick microstrip substrate," *IEEE Trans. Microwave Theory Tech.*, vol. 39, pp. 588–592, Mar. 1991.

[9] S. M. Rao, D. R. Wilton, and A. W. Glisson, "Electromagnetic scattering by surface of arbitrary shape," *IEEE Trans. Antennas Propagat.*, vol. AP-30, pp. 409–418, May 1982.

[10] M. F. Catedra and E. Gago, "Spectral-domain analysis of conducting patches of arbitrary geometry in multilayer media using the CG–FFT method," *IEEE Trans. Antennas Propagat.*, vol. 38, pp. 1530–1536, Oct. 1990.

[11] A. P. M. Zwamborn and P. M. van den Berg, "A weak form of the conjugate gradient FFT method for plate problems," *IEEE Trans. Antennas Propagat.*, vol. 39, pp. 224–228, Feb. 1991.

[12] J. M. Jin and J. L. Volakis, "A biconjugate gradient solution for scattering by planar plates," *Electromag.*, vol. 12, pp. 105–119, 1992.

[13] Y. Zhuang, K. Wu, C. Wu, and J. Litva, "A combined full-wave CG–FFT method for rigorous analysis of large microstrip antenna array," *IEEE Trans. Antennas Propagat.*, vol. 44, pp. 102–109, Jan. 1996.

[14] V. Rokhlin, "Rapid solution of integral equations of scattering theory in two dimensions," *J. Comput. Phys.*, vol. 86, pp. 414–439, Feb. 1990.

[15] V. Jandhyala, E. Michielssen, and R. Mittra, "Multipole-accelerated capacitance computation for 3-D structures in a stratified dielectric medium using in a closed form Green's function," *Int. J. Microwave Millimeter-Wave Computer-Aided Eng.*, vol. 5, pp. 68–78, May 1995.

[16] L. Gurel and M. I. Aksun, "Electromagnetic scattering solution of conducting strips in layered media using the fast multipole method," *IEEE Microwave Guided Wave Lett.*, vol. 6, pp. 277–279, Aug. 1996.

[17] P. A. Macdonald and T. Itoh, "Fast simulation of microstrip structures using the fast multipole method," *Int. J. Numer. Modeling*, vol. 9, pp. 345–357, 1996.

[18] J. S. Zhao, W. C. Chew, C. C. Lu, E. Michielssen, and J. M. Song, "Thin-stratified medium fast-multipole algorithm for solving microstrip structures," *IEEE Trans. Microwave Theory Tech.*, vol. 46, pp. 395–403, Apr. 1998.

[19] C. H. Chan, C. M. Lin, L. Tsang, and Y. F. Leung, "A sparse-matrix/canonical grid method for analyzing microstrip structures," *IEICE Trans. Electron.*, vol. E80-C, pp. 1354–1359, Nov. 1997.

[20] J. R. Phillips and J. K. White, "Precorrected-FFT methods for electromagnetic analysis of complex 3-D interconnect and packages," in *Proc. Progress in Electromag. Res. Symp. Dig.*, July 1995, p. 461.

[21] E. Bleszynski, M. Bleszynski, and T. Jaroszewicz, "A fast integral-equation solver for electromagnetic scattering problem," *IEEE AP-S Int. Symp. Dig.*, pp. 416–419, 1994.

[22] ——, "AIM: Adaptive integral method for solving large-scale electromagnetic scattering and radiation problems," *Radio Sci.*, vol. 31, pp. 1225–1251, Sept.-Oct. 1996.

[23] F. Ling, C. F. Wang, and J. M. Jin, "Application of adaptive integral method to scattering and radiation analysis of arbitrarily shaped planar structures," *J. Electromag. Waves Applicat.*, vol. 12, pp. 1021–1038, Aug. 1998.

[24] D. M. Sheen, S. M. Ali, M. D. Abouzahra, and J. A. Kong, "Application of the three-dimensional finite-difference time-domain method to the analysis of planar microstrip circuits," *IEEE Trans. Microwave Theory Tech.*, vol. 38, pp. 849–857, July 1990.

[25] F. Giannini, R. Sorrentino, and J. Vrba, "Planar circuit analysis of microstrip radial stub," *IEEE Trans. Microwave Theory Tech.*, vol. MTT-32, pp. 1652–1655, Dec. 1984.

[26] T. Edwards, *Foundations for Microstrip Circuit Design*. New York: Wiley, 1991.

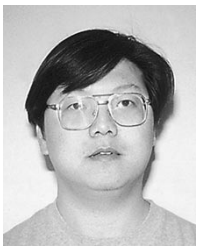

Feng Ling (S'97) was born in Jiangsu, China, in 1971. He received the B.S. and M.S. degrees in electrical engineering from the Nanjing University of Science and Technology, Nanjing, China, in 1993 and 1996, respectively, and is currently working toward the Ph.D. degree in electrical engineering at the University of Illinois at Urbana-Champaign (UIUC).

Since 1996, he has been a Research Assistant at the Center for Computational Electromagnetics (CCEM), UIUC. His research interests include electromagnetic modeling of microwave integrated circuits and microstrip antennas, and fast algorithms for computational electromagnetics.

Mr. Ling is a member of Phi Kappa Phi. He was the recipient of the 1999 Y. T. Lo Outstanding Research Award presented by the Department of Electrical and Computer Engineering, UIUC.

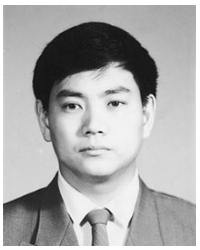

Chao-Fu Wang (M'98) was born on November 15, 1964, in Henan, China. He received the B.Sc. degree in mathematics from the Henan Normal University, Xinxiang, China, in 1985, the M.Sc. degree in applied mathematics from Hunan University, Changsha, China, in 1989, and the Ph.D. degree in electrical engineering from the University of Electronic Science and Technology of China, Chengdu, China, in 1995.

From 1987 to 1996, he was a Lecturer and then an Associate Professor in the Department of Applied Mathematics, Nanjing University of Science and Technology (NUST), Nanjing, China. Since February 1996, he has been an Associate Professor in the Department of Electronic Engineering, NUST. He is currently a Post-Doctoral Research Fellow at the Center for Computational Electromagnetics, University of Illinois at Urbana-Champaign (UIUC). His current research interests include fast algorithms for computational electromagnetics, scattering and antenna analysis, and ferrite components and their analysis.

Jian-Ming Jin (S'87–M'89–SM'94) received the B.S. and M.S. degrees in applied physics from Nanjing University, Nanjing, China, in 1982 and 1984, respectively, and the Ph.D. degree in electrical engineering from The University of Michigan at Ann Arbor, in 1989.

He is currently an Associate Professor of Electrical and Computer Engineering and Associate Director of the Center for Computational Electromagnetics at the University of Illinois at Urbana-Champaign (UIUC). He serves as an associate editor for *Radio Science* and is also on the Editorial Board for the *Electromagnetics Journal* and *Microwave and Optical Technology Letters*. He was the symposium co-chairman and technical program chairman for the 1997 and 1998 International Symposia on Applied Computational Electromagnetics, respectively. He is listed in the UIUC's *List of Excellent Instructors*. He has authored or co-authored over 70 papers in refereed journals and several book chapters. He has also authored *The Finite Element Method in Electromagnetics* (New York: Wiley, 1993) and *Electromagnetic Analysis and Design in Magnetic Resonance Imaging* (Boca Raton, FL: CRC Press, 1998), and co-authored *Computation of Special Functions* (New York: Wiley, 1996). His current research interests include computational electromagnetics, scattering and antenna analysis, electromagnetic compatibility, and magnetic resonance imaging.

Dr. Jin is a member of Commission B of the USNC/URSI, Tau Beta Pi, and the International Society for Magnetic Resonance in Medicine. He served as an associate editor for the IEEE TRANSACTIONS ON ANTENNAS AND PROPAGATION from 1996 to 1998. He was a recipient of a 1994 National Science Foundation Young Investigator Award and the 1995 Office of Naval Research Young Investigator Award. He also received the 1997 Xerox Research Award presented by the UIUC College of Engineering, and was appointed as the first Henry Magnuski Outstanding Young Scholar in the Department of Electrical and Computer Engineering, UIUC, in 1998.